UNITED STATES DEPARTMENT OF THE INTERIOR291
GEOLOGICAL SURVEY

Soil Formation on the Trail Canyon Alluvial Fan, Fish Lake Valley, Nevada

by

Jennifer W. Harden[1], Janet L. Slate[2], Paul Lamothe[1],
Oliver Chadwick[3], Elise Pendall[1], Alan Gillespie[4]

Open File Report 91-291

[1]U.S. Geological Survey, 345 Middlefield Road, Menlo Park, CA 94025; [2]Geology Dept., University of Colorado, Boulder, CO 80309; [3]Jet Propulsion Labs, Oak Grove Ave, Pasadena, CA,91109;[4] Univ. Washington, Seattle, WA 98195

Soil Formation on the Trail Canyon Alluvial Fan, Fish Lake Valley, Nevada

Jennifer W. Harden[1], Janet L. Slate[2], Paul Lamothe[1], Oliver Chadwick[3], Elise Pendall[1], Alan Gillespie[4]

[1]U.S. Geological Survey, 345 Middlefield Road, Menlo Park, CA 94025; [2]Geology Dept., University of Colorado, Boulder, CO 80309; [3]Jet Propulsion Labs, Oak Grove Ave, Pasadena, CA,91109;[4] Univ. Washington, Seattle, WA 98195

Introduction

The Trail Canyon area was selected for a detailed study of soil genesis in the Fish Lake Valley area, because several Holocene and Pleistocene fans exist here (Fig. 1). The fans along Trail Canyon vary in age from about 700 yr to <700,000 yr BP, but clast and matrix lithology, elevation and precipitation, erosional modification, and vegetation also vary among the study sites. We do not consider the age sequence as a soil chronosequence (Jenny, 1941) in which time is the principal cause for differences in soils. Rather, comparisons of these soils comprise a complex story of soil genesis through time, changing climate, and erosional response.

Alluvial fans along Trail Canyon: parent material for Quaternary soils

The bedrock source for alluvium at Trail Canyon and Rock Creek is sharply divided, with granitic rocks in the headwaters region and volcanic rocks in the middle and lower reaches (Crowder and others, 1972; Robinson and Crowder, 1973). A middle to lower basin source for deposits younger than the Trial Canyon unit is indicated by the abundance of volcanic clasts and paucity of granitic clasts. Ratios of volcanic to granitic clasts increase from old to young and west to east, with less than 2:1 on Trail Canyon (surfaces and soils 1 and 2), 3:1 on the early Indian Creek surface (surface/soil 3), and 9:1 on the late Indian Creek surface (surface/soil 4). The change in lithology on the Indian Creek surface (surfaces and soils 3 and 4)

suggests that either the surface is lithologically heterogeneous as a result of depositional or post-depositional processes, or that granitic clasts are sorted with respect to distance from the source. The latter seems unlikely, because such lithologic change is not found on fans from other drainages to the south. As an example of depositional differences, the final depositional pulse that formed late Indian Creek could have been a debris flow lobe headed in the volcanic source area. Alternatively, post-depositional processes may explain the lithologic heterogeneity, as evidenced by a Holocene channel-fill within the late Indian Creek surface.

Alluvial fan deposits in Fish Lake Valley vary from unsorted, bouldery, matrix-supported debris flows to well sorted, pebbly, clast supported fluvial deposits. Most deposits are between the two extremes, existing as moderately sorted, matrix supported deposits. In most exposures, several such deposits occur with few buried soils to indicate significant haituses. Individual debris flows are typically .5 to 1 meter thick and at least 2 meters in length.

The nature of these deposits provides a heterogeneous parent material for soil formation, and in most cases, the boundaries of soil horizons are controlled by the depositional boundaries (for example, 2Bt over 3Bk horizons, meaning Bt formed in deposit number 2 and Bk formed in deposit 3).

We refer to fan deposits and fan surfaces somewhat interchangably, recognizing that the surfaces overlie the deposits and that dates from within the deposits offer a maximum age for the surface. In addition, we refer to (map) units, surfaces, and deposits or alluvium of given nomenclature (for example deposits of Marble Creek or the Marble Creek unit), again recognizing that alluvial deposits comprise the fill underlying the geomorphic surface and mapping unit. Soils formed in such deposits or on such surfaces are referred to as "soil of the given (eg early Marble Creek) unit" or most simply, "the Marble Creek soil".

Site characteristics for the soils study

Site characteristics for the seven fans at Trail Canyon have several variations, some of which covary (Table 1). Holocene and

late Pleistocene soils are developed in gravelly rhyolitic alluvium, whereas the two oldest soils are developed in bouldery granitic outwash. From young to old soils, the elevation generally increases, which causes a shift in temperature, preciptitation, and vegetation. Erosional history, inferred from aerial photographs and field evidence, is somewhat variable, with the surfaces of late (?) Indian Creek (surface and soil 4) and late Trail Canyon (surface and soil 2) exhibiting the greatest local relief, variation in depths to B horizons, and protrusion of weathered boulders above the current surface. Climatic histories of the soils also vary among the sites, in which older soils probably developed through several cycles of effectively drier (interglacial) and wetter (glacial) climatic conditions.

Morphologic and developmental trends with increasing age

Despite the variations of lithology and erosional history among the sites, there is a systematic increase in soil development with age, which covaries with elevation and climate (Table 2, Fig. 2). The most systematic changes with time in soil morphology (Supplementary Table 1) occur in properties related to carbonate content (field carbonate, color paling and lightening, and carbonate stage re Gile and others, 1966; Bachman and Machette, 1977), clay accumulation (total-texture and clay films), and cementation (dry consistence). Carbonate content, discussed below, appears quite variable within a geomorphic unit, especially for eroded soils of surfaces 2 and 4 (Supp. Table 2, field index of carbonate).

Soils at Trail Canyon are generally similar to soils on similar surfaces toward the southern end of the valley (Fig. 3). In several cases, the index numbers are somewhat higher at Trail Canyon than other areas, because these soils were excavated to depths of 3 meters as compared to 1 to 2 meters in other areas. It is interesting to note the systematic increase in development of the Indian Creek soils from McAfee to Furnace Creeks, which might indicate decreasing erosional modification of this unit southward as Pleistocene faulting decreases (see Slate, 1991, this volume).

The rate of development of Holocene soils can be estimated with the use of radiometric dates using an iterative two-error

regression (Switzer and others, 1988). Compared to soils developed near the Silver Lake Playa (Wells and others, 1987; Reheis and others, 1989; Harden and others, 1991), the rates at Trail Canyon are quite similar with respect to both soil morphology (data not shown) and carbonate accumulation (Fig. 4). If most of the carbonate in Holocene soils is derived from eolian dust (Machette, 1985; Gile and others, 1966; McFadden and others, 1987), then these data suggest that late- to middle-Holocene rates of dust-flux are probably similar between the two areas.

Genesis of pedogenic silica, iron, and carbonate

Some of the profiles exibit brittleness or cementation in the field, which we presumed to be some form of secondary silica and/or iron. We therefore extracted iron, aluminum, and silica with sodium dithionite (Jackson, 1965), and subsequently **on the same samples**, extracted these elements with KOH (2.5 minutes boiling; Taylor, 1989). A description of our methods is provided in Suppementary Tables 1.

In principal, dithionite reduces iron oxides (including oxyhydroxides, hydroxides, and oxides) for complexation and analysis. Si and Al species are also extracted by dithionite if they are (1) water soluble (for example monosilicic acid), (2) soluble in weak acid, (3) sorbed by clays or oxides, or (4) structurally bound to dithionite-extractable iron oxides.

Extraction by KOH removes amorphous silica such as volcanic glass and opal, as well as aluminum and other elements associated with the glass (and to a minimal extent, the opal). The ratio of KOH-extractable Si/Al provides a means to detect opaline silica apart from glass, which has molar ratios in excess of about 8 (Chadwick and others, 1987, 1989).

Silica

On samples from many horizons, dithionite removes about the same amount of silica as KOH, generally between about 0.5 and 2 percent of the <2mm fraction. The greatest amounts of dithionite silica, however, are found almost exclusively in Bt and Btq horizons (values greater than about 0.5 percent, Supplementary Table 3),

generally within about 0.5 meter of the surface. The dithionite-extractable silica is probably sorbed to iron (oxy-, hydrous-, and) oxides or to clay, possibly as monosilicic acid polymers (Chadwick and others, 1987).

KOH-extractable silica ranges from 0.2 to almost 2.0 percent. The opal-rich horizons, indicated by KOH-extractable Si/Al ratios greater than 8 to 12, generally occur in the upper 50 to 100 cm and have variable amounts of dithionite iron, silica, and aluminum (Supp. Table 3). In profile 1a and 3a, the two least eroded Pleistocene profiles, the Bq horizons occur at the base of the leached, generally noncalcareous horizons at the surface. It is possible that in less eroded soils, silica is leached like carbonate to depths of average wetting or most frequent leaching.

In Pleistocene soils, there is a systematic increase with depth in the KOH-extractable Si/Al ratio to some maximum value, below which the ratio declines to values similar to the A horizon (Fig. 5b). This Si/Al 'bulge' does not correspond to maximum values of dithionite-extractable Si/Al ratios nor to maximum values of dithionite Fe, Si, or Al (Supp. Table 3). This non-association suggests that the extracts are indeed specific to different forms of Si and Al. For soils included in Supplementary Table 3, the peaks in KOH-extractable Si/Al ratios correspond to maximum values of KOH-extractable Si. In other profiles not shown, the peaks in silica sometimes occur at different depths than the Si/Al peaks. We hypothesize that variations in percent Si and Al values probably indicate variable concentrations of volcanic glass, whereas wide Si/Al ratios probably indicate horizons with opaline silica or monosilicic acid polymers (e.g. excess Si over Al). The predominant source of pedogenic silica appears to be volcanic glass from both rhyolitic alluvium and tephra (both airfall and alluvial), as evidenced by glass in thin sections of Holocene and Pleistocene soils. The glass is quite etched and degraded in the Pleistocene soils. Plagioclase feldspar, however, also appears pitted and etched in thin section and must contribute silica to the pedogenic opal as well.

The amount of opaline silica appears to decrease with age of Pleistocene soils. The soil on late Indian Creek (surface 4) has Si/Al

ratios in excess of 60 (Fig. 5b), wheras the soil on the Trail Canyon surface (surface 1) has ratios of 30. Unfortunately, there is a progression of elevation, climate, vegetation, and lithology that corresponds with age. We hypothesize that the abundance of rhyolite over granite probably most controls the amount of pedogenic opal (highest in surface 4), but the temperature gradient, vegetation composition, and the incidence of airfall tephra probably also play critical roles in the formation of pedogenic opal.

Evidence of pedogenic opal in the Holocene soils is somewhat limited but intriguing. The peaks in KOH-extractable Si/Al ratios (Fig. 5a) occur in all three soils at about 40 to 50 cm depths, which is consistent with that of Pleistocene soils. The increase in the ratio is quite gradual, with a decline below the peak, which also suggests a pedogenic origin. Although molar ratios in excess of about 8 were presumed by Chadwick and others (1987) to be opaline silica, we caution that these soils are abundant in volcanic glass derived from the rhyolitic alluvium and tephra, as evidenced petrographically. Thus further analyses are needed on the abundance and stratification of glass before we can decipher pedogenic opal from inherited glass.

In some cases, we labeled horizons in the field with q for silica before discovering that Si/Al values were not abnormally high. Cementation may require only small amounts of opaline, and iron oxides in these horizons may also play a significant role in the cementation.

Aluminum

In contrast to dithionite-extractable silica, more Al is removed by dithionite than by KOH (Supplementary Table 2; keep in mind that dithionite and KOH extractions are performed in order on the same sample). The most likely source of both forms of pedogenic Al is weathered glass, and it is likely that the dissolved silica from the glass either moves downward as monosilicic acid or precipitates to form amorphous or opaline silica (which are KOH extractable) in the same horizon; by contrast, the Al forms hydrous oxides in place, which is probably extractable by dithionite in association with iron

oxides (see discussion on iron). Hypothetically, KOH-extractable Al might be derived from primary glass.

Iron

Extractable iron appears to be abundant in eolian dust as well as B horizons, as suggested by high dithionite-iron concentrations in Av and B horizons (Supp. Table 3). Zr is also high in A horizons, and eolian dust is probably rich in these components. By contrast, the extractable silica is low in Av horizons, especially in Pleistocene soils, and appears to be mobile relative to Zr and Fe.

The transformations of iron are difficult to track because of the eolian admixtures, but evidence for oxidation of FeO in primary minerals is limited to some of the Pleistocene soils. In profile 1a **(Fig. 6),** the FeO is depleted in the B horizon where dithionite-extractable oxides are more abundant. Barring significant stratification, the Fe/Zr ratios suggest that there is a net gain of Fe in the B horizon relative to the alluvium and possibly to the eolian A horizon. Hypothetically, some iron is probably derived from dust and translocated to the B; as the FeO is not appreciably depleted in the A horizon, most of the dust-derived Fe must be iron hydroxides. McFadden and Hendricks (1985) also documented increases in extractable iron in A and upper B horizons of soils at Cajon Pass, California; they documented tranformation of ferrihydrite to hematite, and hypothesized that the ferrihydrite is formed from weathering of mafic minerals.

It appears that iron oxides act as a substrate for secondary Al and, to a lesser degree, secondary Si. Within Av horizons, pH values are generally buffered by Ca and Na carbonates (pH 8.2 to 8.5), and B horizons commonly have pH values of 7.5 to 8. Laboratory standards of iron oxides generally have no net charge at these pH values (Schwertmann and Taylor, 1989, page 408), thus silica and alumina from weathering of glass would sorb to clays or move to lower horizons with percolating water. Natural samples, the authors note however, are often isoelectrically neutral at lower pH values, so the iron oxides in these horizons might be negatively charged. Silica adsorption onto iron oxides further lowers the isoelectric pH, thus B horizons with more dithionite silica might have more net negative

charge. Aluminum (hydrous) oxides tend to be positively charged in acid pH values (Hsu, 1989), thus concentrations of dithionite silica and aluminum are greatest in B horizons of lower pH values. In Av horizons where pH values are higher, the aluminum hydrous oxides formed from weathering of glass are less likely to be positively charged and may even be mobile, as suggested by lower values of dithionite Al (Supp. Table 3). Alternatively, however, the clays and iron oxides may simply be translocated to B horizons along with sorbed Si and Al.

Carbonate

Carbonate morphology changes systematically over time, with disseminated carbonate in the soils of late Marble Creek (surface 7), powdery undercoats of clasts in the early Marble Creek unit (surface 6), seams and filaments and thicker coatings in Leidy soils, to much denser, thicker coats, and finally massive Bk horizons in the oldest soils (see Pendall and others, this volume). The Bk horizons in the old granitic soils appear less dense than carbonate under rhyolitic clasts of the soils of Indian Creek, and the carbonate percentages are only around 10 percent of the <2 mm fraction (Supp. Table 3).

Despite the systematic changes in carbonate morphology with time, the carbonate concentrations of these soils appear to be quite variable within a given unit, as judged from field indices of carbonate (Table 2; color paling and lightening times carbonate stage; see Harden and others, 1991). For example, percent variability for the field index of carbonate is about 30 to 40 percent (standard deviation divided by the mean of profiles on a given surface), wheras percent variability for total-texture is about 20 percent (calculated from Table 2). Although these field indices are only roughly correlated with mass of carbonate (Reheis and others, in press), the variability is notable. For soil number 4, late (?) Indian Creek, the variability is 70 percent, owing to one profile that has values over 3 times as much carbonate as the other profiles. This profile (4a) contains a K horizon, with a thin argillic horizon on the east side of the pit. The deposit with the K horizon is cut by younger deposits of early Marble alluvium (?), which is surprising because the surface

and varnished pavement appear continual over both deposits. The soil variability of this surface is testimony to its complex erosional history.

The depth to the Bk horizon increases with increasing elevation, which probably indicates an increase in effective wetting. For soils with carbonate analyses (Supp. Table 3), the depth to the Bk ranges from 0 at 5400 feet (profile 7b) to 8 cm at 5475 feet (profile 5c), to 40 cm at 6900 feet (profile 1a). Such a trend was noted by Arkley (1963) for soils along a regional transect of increasing rainfall.

Discussion

Preliminary stages of this study suggest that soil morphology is dramatically influenced by pedogenic iron, silica and carbonate, which in turn are influenced by amount and composition of the dust, composition and coarseness of the parent material, and climatic changes between glacial and interglacial cycles. As a gross generalization, pedogenic iron appears to be derived primarily as iron oxides in dust and is transformed mainly by movement to upper B horizons and possibly by recrystalization in the upper profile (based on McFadden and Hendricks findings, 1985). Some weathering, however, of Fe from primary minerals appears to occur in some B horizons. Pedogenic silica appears to be derived mainly from volcanic glass in alluvium and eolian dust; transformations include sorption to clays in Bt horizons and translocation to greater depths. Opal rich horizons appear to form below Bt horizons but above most of the calcareous horizons. Pedogenic carbonates also are derived primarily from eolian dust, but depth of leaching is much greater for carbonate than clay, iron, or silica.

Clay, iron and silica appear to have much shallower depths of translocation than carbonate, which hypothetically could be related to (1) higher sorption potential related to negative or variable charge of clay, iron and silica (2) transport as colloids and particles rather than dissolved ionic species (3) differing stabilities of the constituents and thus differing responses to erosional and/or climatic changes. For example, water-soluble monosilicic acid may move with saturated wetting fronts, similar to carbonate. Subsequent drying of

the silica, however, can result in the formation of opaline silica, which because of its O bond to other silica groups does not rewet nor remobilize upon rewetting (Chadwick and others, 1987). By contrast, carbonate is much more likely to dissolve and remobilize upon rewetting. As a result, infrequent, extreme wetting events on average tend to separate the depths of the Bk horizons below the depth of the Bq horizons. Such a separation requires formation of opaline silica and is more likely to be observed in older soils, because (1) opal occurs in relatively low abundance in young, Holocene soils and (2) young soils have been subjected to fewer wetting events.

Acknowledgements

Many thanks to the many helpers in the field, including Gregg Vick, Taryn Lindquist, Marith Reheis, Bud Burke and his many students. Also thanks to A. Sarna-Wojcicki for tephra analyses and to Sue Trumbore for charcoal analyses. This work was supported in part by NASA's Land Processes Branch.

References

Arkley, R.J., 1963. Calculation of carbonate and water movement in soil from climatic data. Soil Science 96:239-248.

Bachman, G.O., and M.N. Machette, 1977. Calcic soils and calcretes in the southwestern United States. U.S. Geological Survey Open-File Report 77-794:163.

Chadwick, O.A., D.M. Hendricks, and W.D. Nettleton, 1987. Silica in duric soils. I. A depositional model. Soil Sci. Soc. Amer. Jour. 51:975-982.

Chadwick, O.A., D.M. Hendricks, and W.D. Nettleton, 1989. Silicification of Holocene soils in northern Monitor Valley, Nevada. Soil. Sci. Soc. Amer. Jour. 53:158-164.

Crowder, D.F., P.T. Robinson, D.F. Harris, 1972. Geologic map of the Benton Quadrangle, Nevada. USGS GQ 1013, 1:62,500.

Gile, L.H., F.F. Peterson, and R.B. Grossman, 1966. Morphological and genetic sequences of carbonate accumulation in desert soils. Soil Science 101:347-360.

Gillespie, A.M., 1991. Trail Canyon fans: Capture history of Rock Creek. Guidebook, Pacific Cell, Friends of the Pleistocene, this volume.

Harden, J.W., 1982. A quantitative index of soil development from field descriptions: Examples from a chronosequence in central California. Geoderma 28:1-28.

Harden, J.W. and E.M. Taylor, 1983. A quantitative comparison of soil development in four climatic regimes: Quaternary Research 20:342-359.

Harden, J.W., E.M. Taylor, Cindy Hill, R.K. Mark, L. D. McFadden, M.C. Reheis, J.M. Sowers, 1991. Rates of soil development from four soil chronosequences in the southern Great Basin. Quaternary Research in press.

Hsu, P.H., 1989. Aluminum oxides and oxyhydroxides. In Dixon, J.B. and S.B. Weed (eds.), Minerals in soil environments: Soil Science Soc. Amer., Madison, Wisc.

Jackson, M.L., 1965. Free oxides, hydroxides and amorphous alumino-silicates. In Black (ed.), Methods of soil analysis, Part 1. Agronomy 9:578-603.

Janitzky, Peter, and M.J. Singer, 1986. Field and laboratory procedures used in a soil chronosequence study. U. S. Geological Survey Bulletin 1648, 49 p.

Jenny, Hans, 1941. Factors of soil formation. New York, McGraw-Hill. 281 p.

Machette, M. N., 1985. Calcic soils of the southwestern United States. In D.L. Weide (ed.) Soils and Quaternary geomorphology of the southwestern United States. Geol. Soc. Amer. Special Paper 203, p. 1-21.

McFadden. L.D. and D.M. Hendricks, 1985. Changes in the content and composition of pedogenic iron oxyhydroxides in a chronosequence of soils in southern California. Quaternary Research 23:1890-204.

McFadden, L.D., S.G. Wells, and M.J. Gercinovich, 1987. Influences of eolian and peogenic processes on the origin and evolution of desert pavements. Geology 15:504-508.

Pendall, E.G., J.W. Harden, and S. Trumbore, 1991. Pedogneic isotopic indicators of climate and carbon cycling in Fish lake Valley, Nevada. U.S. Geological Survey Open-file report 91- and Guidebook, Pacific Cell, Friends of the Pleistocene, this volume.

Reheis, M.C., and T. McKee, 1991. Late Cenozoic history of slip on the Fish Lake Valley fault zone, Nevada and California. U.S. Geological Survey Open-file report 91-290, and Guidebook, Pacific Cell, Friends of the Pleistocene, this volume.

Reheis, M.C., J.W. Harden, L.D. McFadden, and R.R. Shroba., 1989. Development rates of late Quaternary soils, Silver Lake Playa, California. Soil Sci. Soc. Amer. Jour. 53:1127-1140.

Reheis, M.C., J.M. Sowers, E.M. Taylor, L.D. McFadden, and J.W. Harden, in press. Mrophology and genesis of calcic soils on the Kyle Canyon Fan, Nevada, USA. Geoderma

Robinson, P.T. and D.F. Crowder, 1973. Geol map of the Davis Mountain Quadrangle, Nevada and California, U.S. Geological Survey map GQ-1078. 1:62,500.

Schwertmann, U. and R.M. Taylor, 1989, Iron Oxides. In Dixon, J.B. and S.B. Weed (eds), Minerals in soil environments. Soil Science Soc. Amer., Madison, Wisc.

Slate, J.L., 1991. Quaternary stratigraphy, geomorphology and geochronology of alluvial fans, Fish Lake Valley, Nevada and California. Guidebook, Pacific Cell, Friends of the Pleistocene, this volume.

Switzer, P.S., Harden, J.W. and Mark, R.K. (1988). A statistical method for estimating rates of soil development and ages of geologic deposits: a design for soil-chronosequence studies. Mathematical Geology 20:49-61.

Taylor, E.M.,1989. Impact of time and climate on Quaternary soils in the Yucca Mountain area of the Nevada Test Site. unpublished masters thesis, University of Colorado, Boulder, 215 p.

Wells, S.G., L.D. McFadden, and J.C. Dohrenwend, 1987. Influence of late Quaternary climatic changes on geomorphic and pedogenic processes on a desert piedmont, eastern Mojave Desert, California. Quaternary Research 27:130-146.

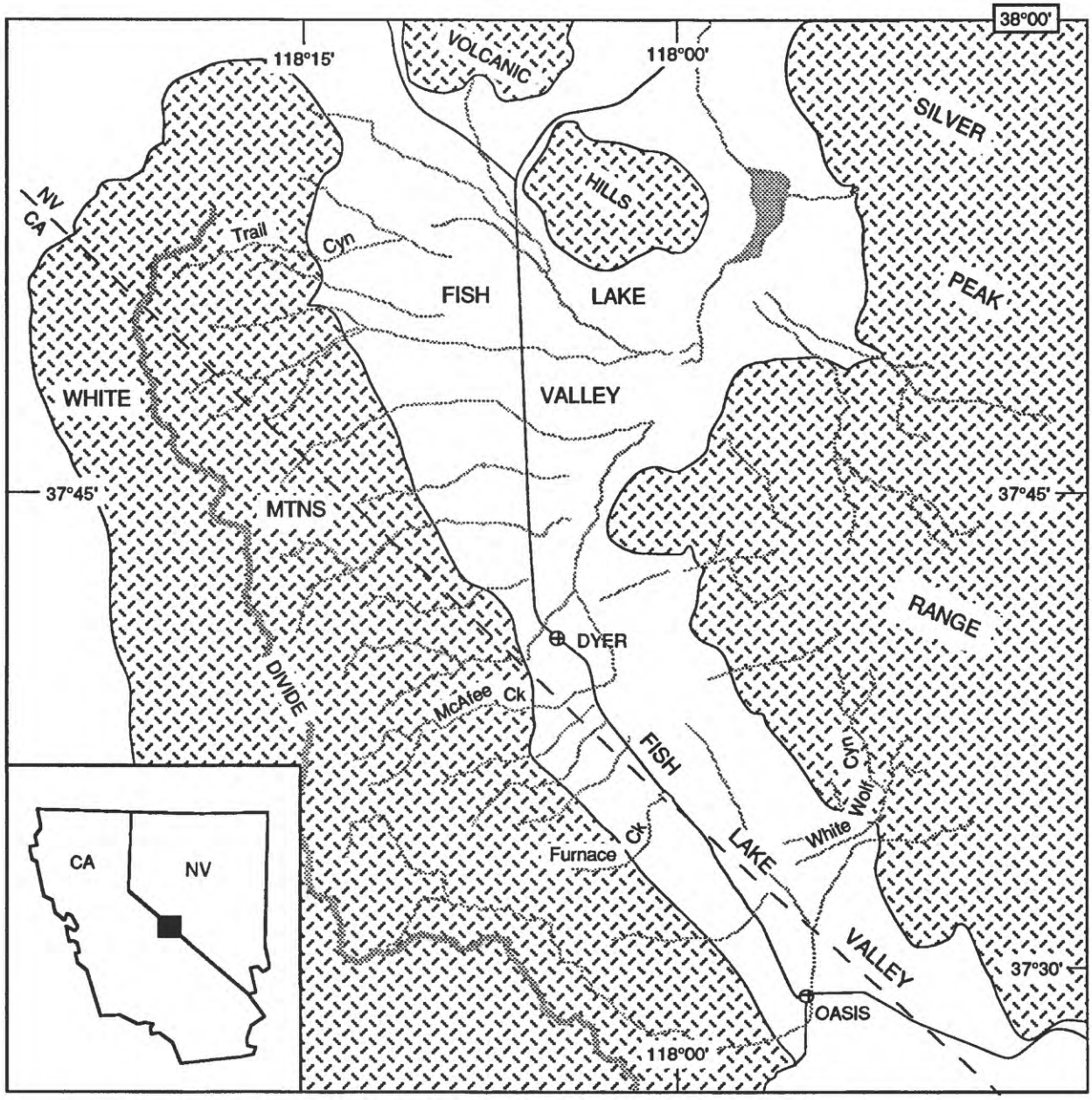

Figure 1A. Map of the Fish Lake Valley area.

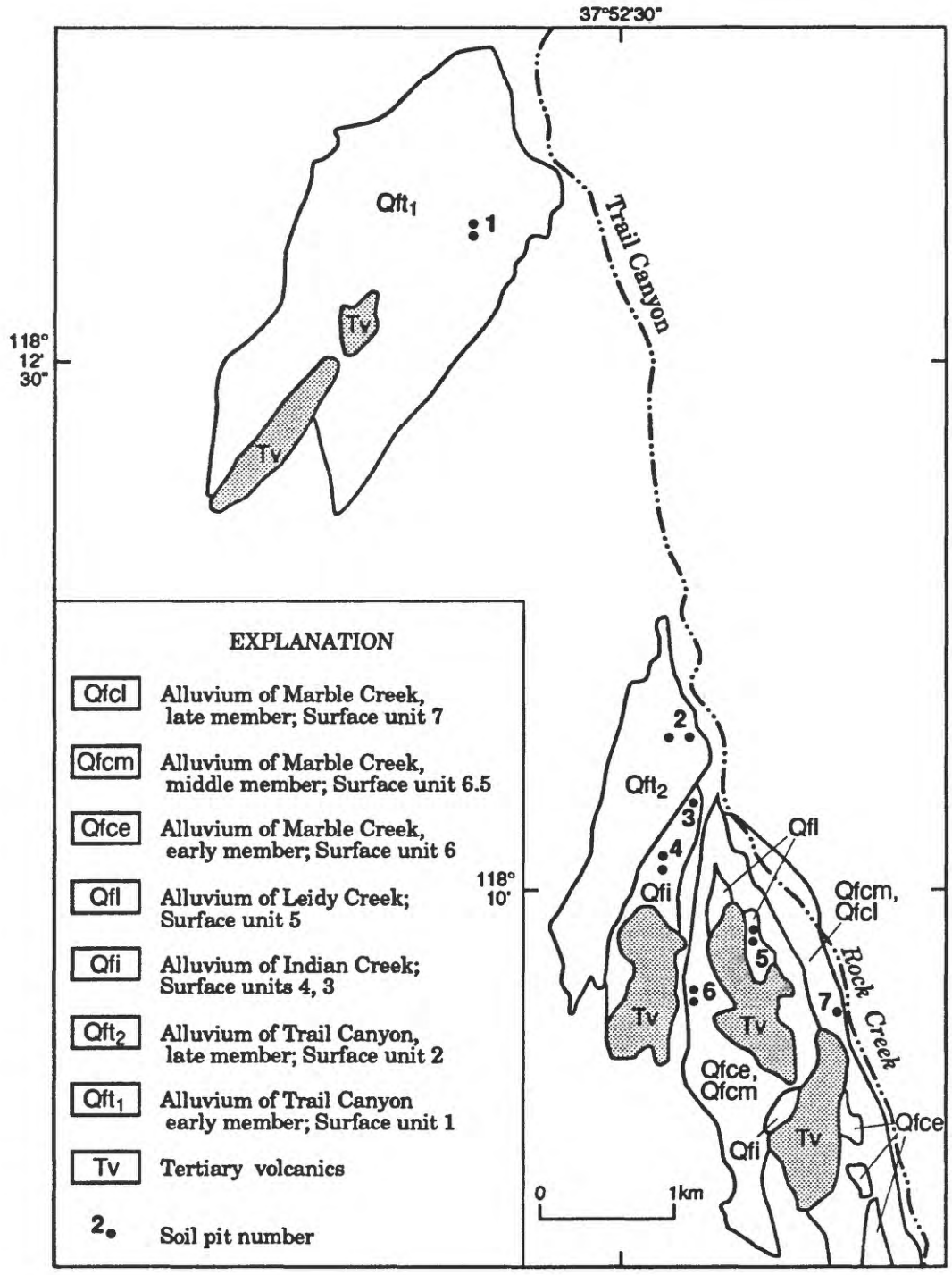

Fig. 1b. Trail Canyon alluvial fans, showing major map units and location of soil pits , adapted from Gillespie (this volume) using nomenclature of Reheis (this volume). X, soil pits and numbers corresponding to tables, figures, and surfaces referred to in text..

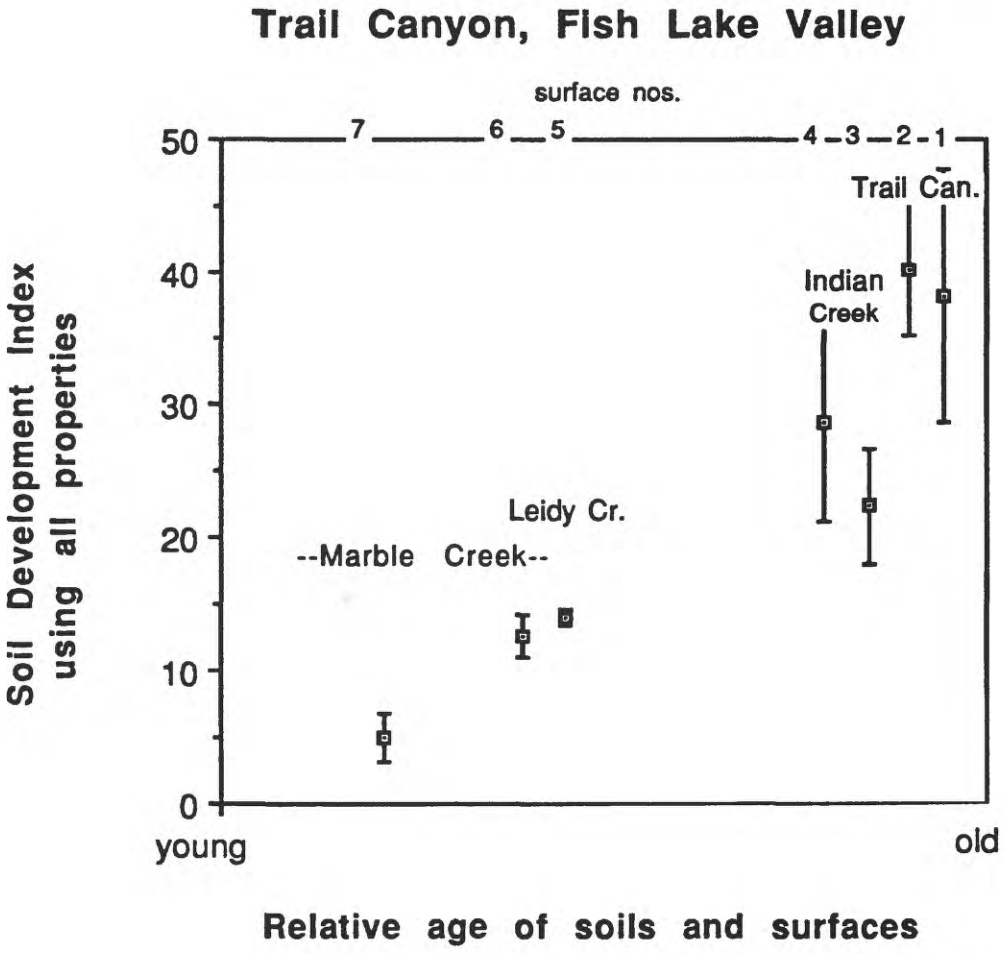

Fig. 2. Soil development index versus relative age for soils at Trail Canyon. Index using all properties (Harden, 1982) shown in Supp. Table 2. Boxes, mean value of replicate sites on fan; vertical bars, standard deviation of replicate sites. Sites shown in fig. 1; data shown in table 2.

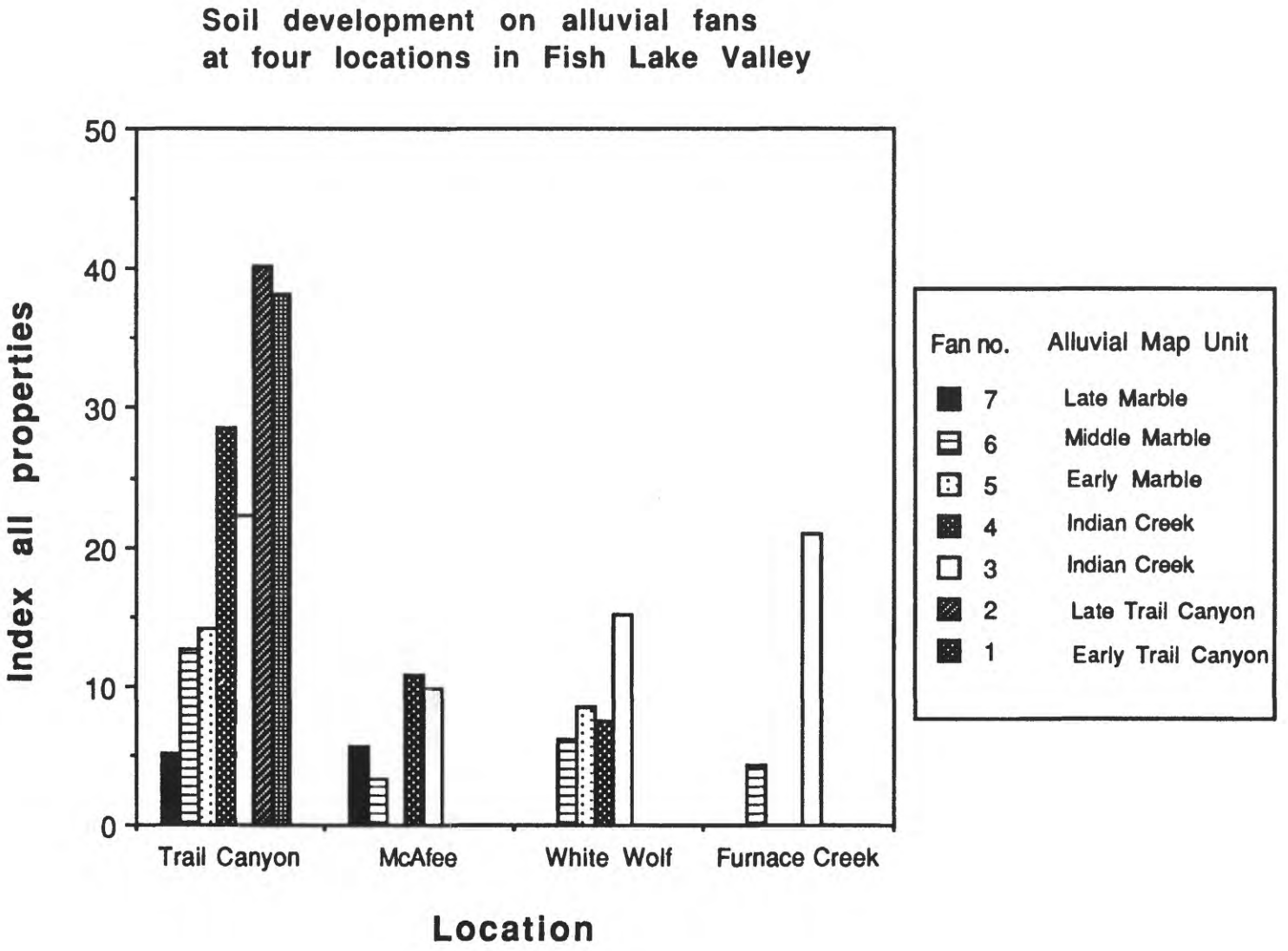

Fig. 3. Soil development index on major map units at Trail Canyon, McAfee Creek, White Wolf, and Furnace Creek. Data from Supp. Table 2 (Trail Canyon) and Slate (this volume).

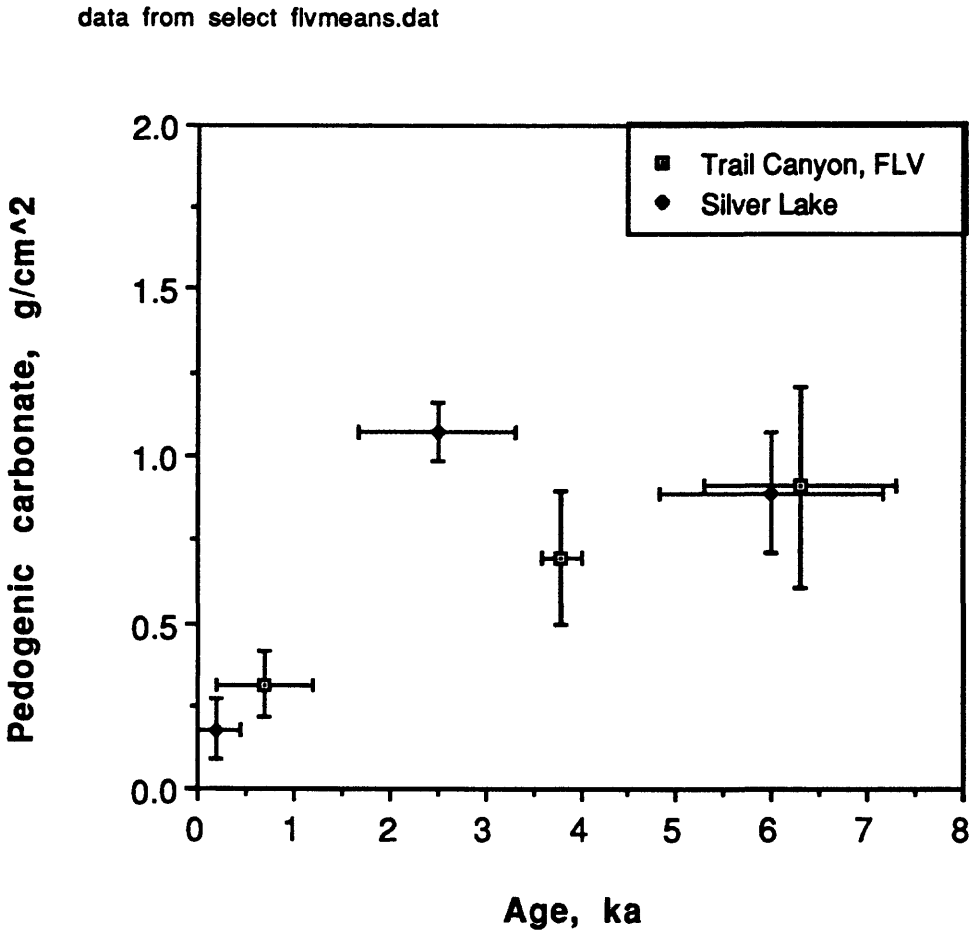

Fig. 4. Carbonate mass versus age for soils at Trail Canyon and Silver Lake. Dots, mean mass for soil replicates of given age and age of surface determined from radiometric dating methods (see text). Vertical bars, standard deviation of soil replicates; horizontal bars, age uncertainty. Carbonate calculated from product of percent of <2mm soils X bulk density X horizon thickness; product summed over profile.

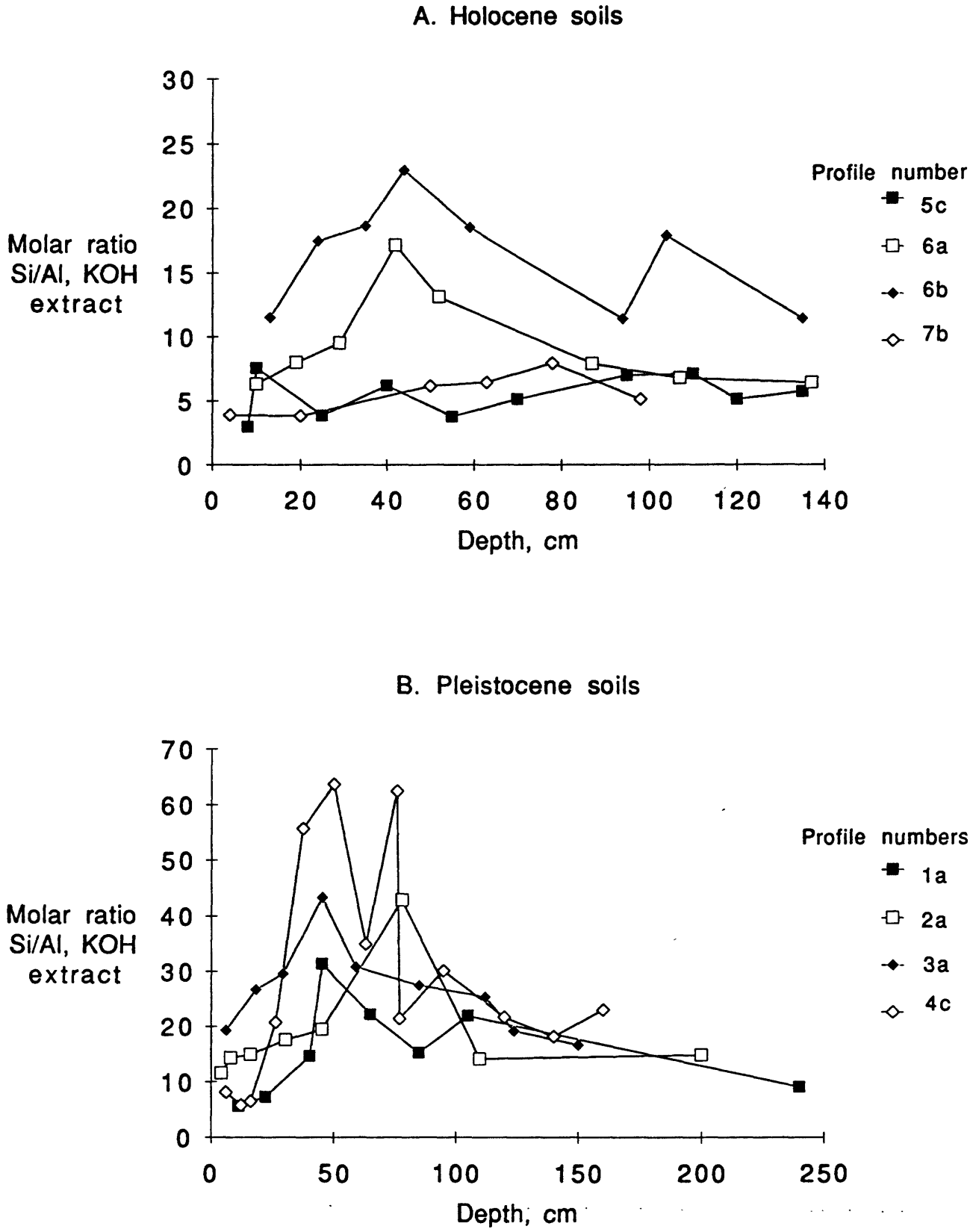

Fig. 5. Molar ratio of KOH-extractable SiO2/Al2O3 for Holocene (a) and Pleistocene (b) soils. Data from Supp. Table 3 converted to molar ratio and from unpublished data.

gb-fig6.fe1a

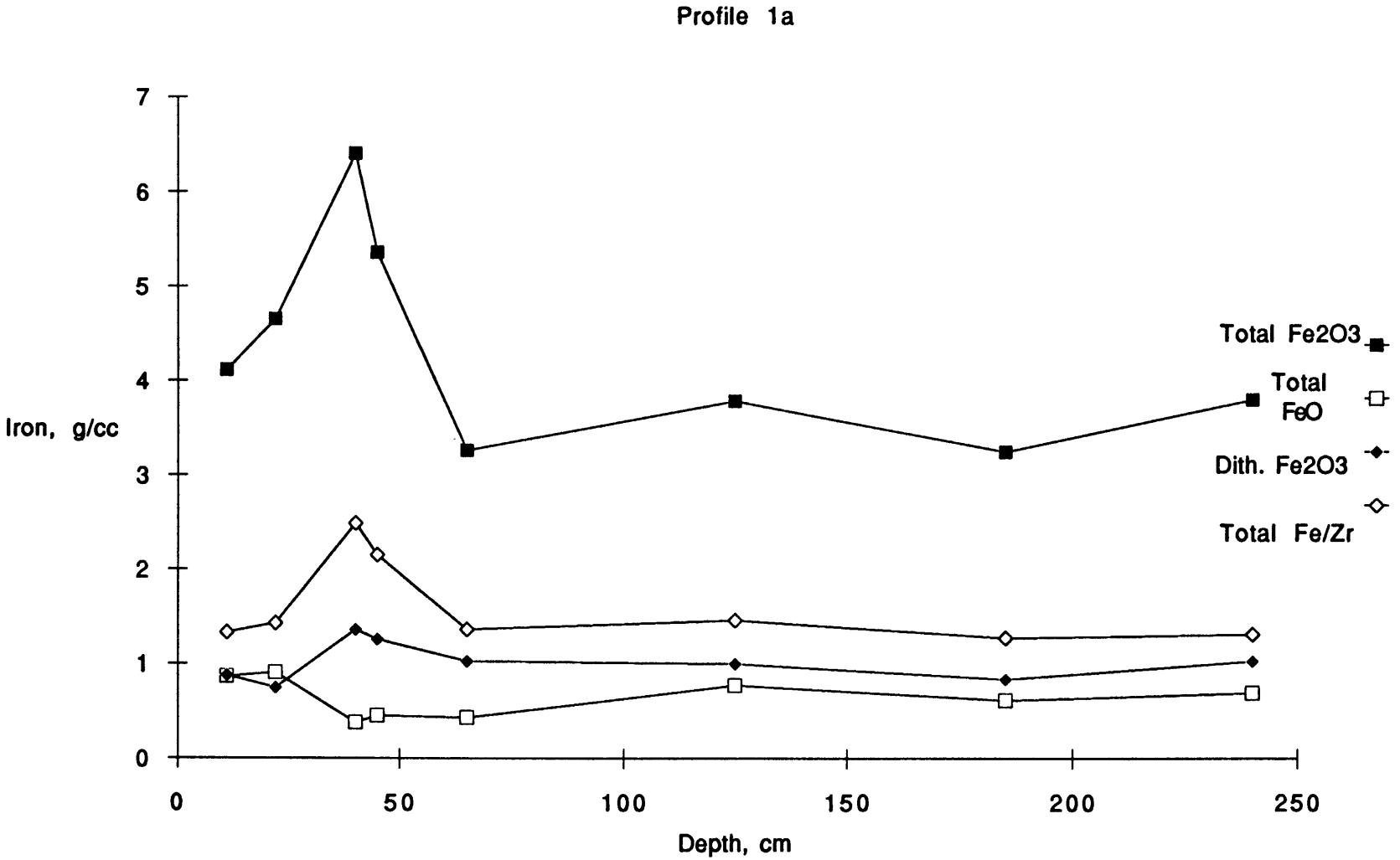

Fig. 6. Various forms of iron versus depth for profile 1a. Data from Supp. Table 3 and unpublished data.

Table 1. Site characteristics for soils at Trail Canyon

Soil number	map unit	Age, ka	Lithology	Erosion	Elevation feet	Inferred MAP, cm	Vegetation
Qf1	Trail Canyon, early member	< 700[1]	Bouldery, granitic	Slight	6900	17-20	Sage, Pinyon Juniper
Qf2	Trail Canyon, late member	< 700[1]	Bouldery granitic	Moderate	5720		
Qf3	Indian Creek early member?	> 40[2] < 700[1]	Gravelly rhyolitic	Moderate?	5630		
Qf4	Indian Creek, late member?	> 40[2] < 700	Gravelly rhyolitic	Moderate	5580	est. 15	Atriplex, grass, etc.
Qf5	Leidy Creek	6.3[3]	Gravelly rhyolitic	Minimal	5475		
Qf6	Marble Creek, early member	3.8[4]	Gravelly rhyolitic	Minimal	5435		
Qf7	Marble Creek, late member	1.0[5]	Gravelly rhyolitic	Minimal	5400	est. 14	Atriplex, grass, etc.

[1] Post-dates tephra of one of the Glass Mountain series

[2] Thermoluminescence on buried A horizon, Univ. Colo. Lab

4 Tephra 141 and 135; C-14 on charcoal LL-

3 C-14 on charcoal at 95 cm depth; QL-4369

5 Composite C-14 on charcoal 2m depth; TO1668

Table 2. Selected profile properties of the soil development index (Harden, 1982) for soils at Trail Canyon

PROFILE	RUBIFICATION	CARBONATE INDEX	TOTAL-TEXTURE	DRY CONSIS-TENCE	CLAY FILMS	INDEX ALL PROPS
1a	24.74	98.44	34.50	66.10	8.08	36.32
1b	20.29	127.06	27.00	70.10	10.15	50.05
1c	13.53	92.08	19.11	72.10	25.69	39.85
1d	20.68	49.13	28.17	41.85	18.46	26.59
2a	20.34	83.98	21.56	50.30	15.54	34.83
2b	14.08	99.43	16.67	57.50	7.69	41.36
2c	17.16	74.00	25.11	56.60	6.77	44.54
3a	14.79	19.76	20.11	18.30	2.54	17.98
3b	16.26	29.33	27.33	39.75	8.00	26.60
3c	14.39	24.71	16.67	32.90	15.00	22.43
4a	11.89	71.19	14.44	67.40	3.00	35.22
4b	28.20	23.79	36.11	40.95	5.08	30.08
4c	13.00	22.27	11.33	36.80	11.00	20.52
5a	11.58	14.83	13.33	15.60	9.92	14.51
5b	9.47	7.83	18.56	19.80	4.58	14.34
5c	11.05	12.27	12.78	19.00	0.00	13.35
6a	6.63	13.71	7.11	21.40	2.31	14.38
6a	7.76	16.35	3.78	21.90	2.12	11.90
6c	6.63	12.52	18.67	20.80	2.31	11.44
6.5a	1.97	18.25	10.22	24.25	0.00	12.39
7a	0.16	0.00	3.11	10.70	0.00	3.81
7b	0.00	0.08	8.78	13.70	0.00	6.36

Supplementary Table 1. Laboratory Methods for extractive chemistry

Citrate-Bicarbonate-Dithionite (CBD) extraction of Fe, Al, and Si

The procedure used for citrate-bicarbonate-dithionite (CBD) extractable iron, aluminum, and silicon was a slight modification of the procedure published by Janitzky (USGS Bulletin 1648, pp. 38-41). We used 1.00-g soil samples, ground to -100 mesh, and scaled-down the volume of reagents used accordingly (see attached step-by-step procedure for details). The most important departure we made from previous studies was our use of inductively-coupled plasma atomic emission spectrometry (ICP-AES) for the final elemental determinations. ICP-AES is superior to atomic absorption spectrometry (AAS) is three respects: a) ICP-AES has significantly lower detection limits for Si and Al compared to AAS, b) ICP-AES is far less sensitive to matrix effects than AAS, and c) ICP-AES is a multi-element technique. Because of these advantages, we were able to measure extractable Fe, Al, and Si simultaneously in the CBD extraction solutions which eliminated the need for: 4 evaporation steps, a precipitation step, a separation step, a precipitate-digestion step, a dilution step, and a filtration step. Accuracy and precision were also improved because of the reduced amount of sample handling. Precision was typically better than 4% RSD, and the detection limits for Fe, Al, and Si were 1, 15, and 5 μg/g respectively in the soil samples.

Procedure for Dithionite Extractable Fe, Al, and Si

1. Prepare a water bath at 75° C (maximum 80° C) using a large open pan on a suitable hotplate with one or two plastic test tube racks. The level of water in the pan must be high enough to cover approximately 15 ml contained in the centrifuge tubes as they sit in the racks.

2. Place 1.00 g soil samples, ground to pass an 80 mesh sieve, into eight 50 ml conical bottom centrifuge tubes. Place the eight tubes in a plastic test tube rack, and place the rack in the water bath. Add an extra tube with about 15 ml water and a thermometer to serve as a temperature sensor.

3. Using a dispensing pipette, add to each tube 10 ml of 0.3 M sodium citrate and 1.25 ml of 1 M sodium bicarbonate. Mix suspensions with glass rods, leaving rods in tubes.

4. When the temperature of the sensor tube has reached 70-75° C., add about 0.25 g sodium dithionite powder to the first sample with a spatula, stir briskly for one minute with the glass rod, (use a timer) and continue to the next sample in a similar manner. Do not allow the temperature to exceed 80° C. A second addition of dithionite is made as soon as the eighth sample has been treated. Allow the suspensions to digest, with intermittent stirring, for a minimum of 15 minutes.

5. Add to each sample 1.25 ml of saturated NaCl solution (12.5 ml syringe), stir the suspension and remove the stirring rod, rinsing with deionized water from a washbottle.

6. Centrifuge samples at 1600-1800 RPM until clear supernatant is obtained (2-5 minutes). Collect solutions in 100 ml volumetric flasks.

7. Repeat digestion procedure in an identical manner (steps 3, 4, 5, and 6).

8. After collection of the second extract, add to each tube 10 ml sodium citrate solution and 1.25 ml saturated NaCl solution. Stir by swirling. Centrifuge. (Centrifuging the samples at this stage may occasionally take longer to settle the suspension than was required in the previous steps. The organic matter content appears to influence the suspension. Samples from lower horizons usually need the least centrifuging time.

9. Collect supernatants in volumetric flasks and wash samples with citrate and NaCl a second time. Make solutions to volume with deionized water.

10. Determine Fe, Al, and Si using ICP-AES. Use the 259.94 nm Fe line calibrated over the range of 0-70 ppm Fe; use the 308.21 nm Al line calibrated over the range of 0-10 ppm Al; and use the 251.61 Si line calibrated over the range 0-30 ppm Si. Prepare the aqueous calibration solutions in a citrate-bicarbonate-dithionite matrix that matches the sample solutions.

Procedure for KOH Extractable Al and Si

1. Following the dithionite extraction procedure, add 15 ml of deionized water to each residue, shake well, centrifuge, and discard the rinse water.

2. Add 15 ml of 0.5 M KOH to each residue, and heat the loosely-capped samples (3 at a time) in a microwave oven for 45 seconds (in order to rapidly heat the samples to approximately 90° C). Immediately following the microwave heating step, place the samples in a boiling water bath for exactly 2.5 minutes, and then quench the reaction by placing the vials in a cold water bath until cool to the touch.

3. Centrifuge each sample at 1600-1800 rpm for 2.5 minutes, decant the supernatant liquid into a 25 ml volumetric flask and dilute to volume with water.

4. Determine Al and Si concentrations using ICP-AES. Use the 251.61 nm Si line, calibrated over the range of 0-200 ppm Si, and use the 308.21 Al line calibrated over the range of 0-40 ppm Al. Prepare aqueous calibration solutions in a KOH matrix that matches the sample solutions.

Procedure for Carbonate Carbon

A 0.1-g sample is digested with 2 mL of 2M perchloric acid, and the carbon dioxide evolved is collected in a coulometric cell, where it is converted to a strong titrable acid by ethanolamine. The acid is titrated automatically with coulometrically generated base and the endpoint is detected colorimetrically. The detection limit using this sample size is 0.02% carbon, and the precision is typically 3-4% RSD. Reagent grade Na_2CO_3, and the international geologic reference material, SCo-1, were run with each batch of samples as quality control checks.

SUPPLEMENTARY TABLE #2

FIELD MORPHOLOGY

Profile	Horizon	Base (cm)	Dry Color	Moist Color	Texture	Stucture Grade	Stucture Kind	Consistence Dry	Consistence stkn	Consistence plst	CaCO3 STAGE	pH
FLVTC1a	A1	11	2.5Y 7 3	10YR 4 3	SL	v.wk	Sbk	v so	so	po	0	7.2
	A2	22	2.5Y 7 3	10YR 5 4	SL	wk	Sbk	so+	ss	ps	0	7.4
	Bt1	40	7.5YR 6 6	7.5YR 5 6	CL	mod	sg/m	h	s	vp	0	7.2
	Bt2	45	10YR 7 6	10YR 5 6	SCL	mod	Sbk	h	vs	p	0	7.2
	2Bk1	60	2.5Y 8 3	2.5Y 7 4	vgLS	v.wk	sg/m	h	so	po	2.5	8
	2Bk2	240	2.5Y 8 3	2.5Y 6 4	gLS	v.wk	sg/m	h	vss	po	2	8.2
FLVTC3a	Av	6	2.5Y 6 2	10YR 5 3	sl	mod	m/sbk	sh	ss	ps	0.5	7
	Bw	18	7.5YR 5 4	7.5YR 4 4	l	wk	Sbk	so	ss	ps	0	999
	Btq	29	7.5YR 5 6	7.5YR 4 6	nd	str	Sbk	eh			0	999
	2Bqk1	45	7.5YR 7 3	7.5YR 5 4	nd	mod	m/sbk	vh			3	999
	3Bk2	59	10YR 7 3	10YR 4 4	sl	v.wk	sg/m	so	so	po	1	999
	3Bk3	85	10YR 7 4	10YR 5 4	sl	v.wk	sg/m	so	ss	ps	1	999
	3Bk4	112	10YR 7 3	10YR 5 3	sl	v.wk	sg/m	lo	ss	ps	1	999
	4Bk5	124	10YR 6 3	10YR 4 3	sl	v.wk	sg/m	lo	so	po	1	999
	5Bb	150	7.5YR 7 4	10YR 5 4	l	wk	Sbk	sh	ss	ps	1	999
FLVTC4c	A	6	10YR 7 3	10YR 5 3	sl	wk	Sbk	so	so	po	0	999
	Av1	12	10YR 7 3	10YR 5 4	sl/l	wk	Sbk	so	ss	ps	0	999
	Av2	16	10YR 7 2	10YR 5 4	l	mod+	m/sbk	h	s	p	0.5	999
	2Bktq1	26	10YR 8 3	10YR 5 4	l	wk	Sbk	vh	s	p	0.5	999
	2Bktq2	37	7.5YR 5 6	7.5YR 4 6	nd	str	m/sbk	eh			2	999
	2Btkqm3	50	7.5YR 7 6	7.5YR 5 6	nd	str	m/sbk	eh			1	999
	3Bkqm4	63	7.5YR 8 2	7.5YR 8 1	nd	str	m/sbk	eh			2	999
	4Bk5	76	7.5YR 8 2	7.5YR 7 4	l	v.wk	sg/m	so+	so	po	2	999
	Avb	77										
	4Bk6	95	10YR 7 3	10YR 5 4	l	v.wk	sg/m	so+	ss	ps	1	999
	5Bk7	120	7.5YR 7 4	7.5YR 6 4	l	v.wk	sg/m	so+	so	po	1	999
	5Bk8	140	7.5YR 7 4	7.5YR 6 4	l	v.wk	sg/m	so+	ss	ps	1	999
	6Bk9	160	7.5YR 8 2	7.5YR 7 4	sl	v.wk	sg/m	sh+	ss	po	0.5	999
	6B10	170	7.5YR 7 2	7.5YR 4 4	l	v.wk	sg/m	so+	ss	ps	0	999
FLVTC5c	Av1	8	10YR 7 2	10YR 4 3	l	mod	Sbk	sh	vss	po	0	8.2
	Av2	10	10YR 7 2	10YR 4 3	l	mod	Sbk	sh	vss	po	0.5	8.2
	2Btj	25	10YR 7 3	10YR 4 4	l	wk	Sbk	so	so	po	0.5	7.6
	3Btjk	40	10YR 6 3	10YR 4 4	sl	wk	Sbk	so	so	po	1	7.6
	4Bk1	55	10YR 7 4	10YR 4 4	ls	wk	Sbk	sh	so	po	1	7.6
	5Bk2	70	10YR 6 3	10YR 4 3	ls	wk	Sbk	sh	so	po	1	8
	6BCk	95	10YR 6 3	10YR 4 4	ls	wk	Sbk	sh	so	po	1	8.2
	7CB	110	10YR 6 3	10YR 4 4	ls	v.wk	sg/m	lo	so	po	0.5	8.2
	8C	120	10YR 6 3	10YR 4 4	ls	v.wk	sg/m	lo	so	po	0.5	7.6
	9Bb	135	10YR 7 3	10YR 4 6	l	wk	Sbk	sh	ss	po	0.5	7.6
FLVTC6a	Av	10	2.5Y 7 3	10YR 4 3	L	wk	m/sbk	so	so	po	0	8.2
	Bw	19	2.5Y 7 3	2.5Y 5 3	SL	wk	Sbk	so	ss	po	0.5	8.2
	Bt	29	10YR 7 4	10YR 5 4	SL	wk	Sbk	so	ss	po	0.5	8.2
	Bk1	42	2.5Y 8 3	10YR 5 4	coSL	wk	Sbk	so	so	po	1	8.2
	2Bk2	52	2.5Y 8 3	10YR 5 4	coSL	v.wk	sg/m	lo	so	po	1	8.3
	3Bz	87	2.5Y 8 2	10YR 4 4	SL	wk	Sbk	h	ss	po	1	8.3
	Tephra	89								po		999
	4Bwb	107	10YR 7 3	10YR 4 4	SL	wk	Sbk	sh	ss	po	0.5	8.3
	5BC	137	2.5Y 8 2	10YR 4 4	coSL	v.wk	sg/m	lo	so	po	0.5	999
FLVTC7b	A	4	10YR 6 3	10YR 4 3	sl	wk	m/sbk	so	vss	po	0.5	999
	2C1	20	10YR 7 3	10YR 5 4	sl	wk	Sbk	so	ss	ps	0	999
	3C2	50	10YR 7 3	10YR 5 4	sl	wk	Sbk	so	ss	po	0	999
	4C3	63	10YR 7 3	10YR 5 4	sl	v.wk	sg/m	so	so	po	0	999
	5C4	78	10YR 7 3	10YR 5 4	sl	v.wk	sg/m	so	ss	po	0	999

SUPPLEMENTARY TABLE #3

EXTRACTABLE CHEMISTRY

Profile	horizon	base	%CaCO3	Fe2O3-d	SiO2-d	SiO2-KOH	Al2O3-d	Al2O3-KOH	SiO2/Al2O3 KOH extract	SiO2/Al2O3 KOH, molar ratio
			subsoil maximum highlighted in bold							
FLVTC1a	A1	11	0.000	0.598	0.257	0.207	0.092	0.063	3.307	5.620
	A2	22	0.000	0.496	0.261	0.244	0.073	0.057	4.287	7.285
	Bt1	40	0.000	**0.826**	**0.646**	0.845	**0.191**	**0.098**	8.632	14.668
	Bt2	45	0.417	0.720	0.610	**1.239**	0.139	0.067	**18.462**	**31.374**
	2Bk1	65	0.417	0.569	0.385	0.355	0.054	0.027	13.049	22.175
	2Bk2	125	2.250	0.554	0.304	0.116	0.048	0.013	8.950	15.209
	2Bk2	185	**6.583**	0.464	0.270	0.145	0.037	0.011	12.915	21.947
	2Bk2	240	1.080	0.546	0.250	0.066	0.046	0.012	5.309	9.021
FLVTC3a	Av	6	3.250	1.047	0.359	0.672	0.098	0.059	11.356	19.298
	Bw	18	0.000	0.966	**0.575**	1.048	**0.133**	**0.067**	15.669	26.626
	Btq	29	0.000	0.856	0.522	0.958	0.088	0.055	17.427	29.614
	2Bqk1	45	2.833	0.710	0.458	**1.219**	0.073	0.048	**25.503**	**43.338**
	3Bk2	59	3.833	0.674	0.404	0.759	0.069	0.042	18.183	30.900
	3Bk3	85	**4.333**	0.718	0.430	0.597	0.070	0.037	16.196	27.522
	3Bk4	112	3.250	**0.780**	0.415	0.599	0.074	0.040	14.951	25.406
	4Bk5	124	0.917	0.728	0.312	0.355	0.058	0.031	11.320	19.236
	5Bb	150	0.333	0.613	0.299	0.430	0.069	0.044	9.765	16.594
FLVTC4c	A	6	0.250	0.768	0.282	0.280	0.098	0.059	4.784	8.129
	Av1	12	0.000	0.767	0.257	0.229	**0.106**	0.067	3.422	5.814
	Av2	16	0.333	0.888	0.293	0.259	0.104	**0.068**	3.815	6.483
	2Bktq1	26	4.000	**0.898**	0.428	0.755	0.098	0.062	12.220	20.766
	2Bktq2	37	**5.917**	0.753	0.554	**1.803**	0.081	0.055	32.792	55.725
	2Btkqm3	50	0.750	0.752	**0.582**	1.769	0.076	0.047	**37.446**	**63.633**
	3Bkqm4	63	2.333	0.551	0.501	0.873	0.061	0.042	20.618	35.037
	4Bk5	76	**13.667**	0.387	0.449	0.757	0.053	0.021	36.763	62.473
	Avb	77	3.667	**0.635**	0.389	0.460	0.069	0.036	12.610	21.429
	4Bk6	95	9.917	0.565	0.443	0.674	0.066	0.038	17.740	30.146
	5Bk7	120	5.583	0.600	0.334	0.280	0.061	0.022	12.784	21.724
	5Bk8	140	1.833	0.790	0.338	0.263	0.071	0.025	10.710	18.200
	6Bk9	160	1.167	0.806	0.355	0.421	0.071	0.031	13.515	22.967
	6B10	170	nd	nd	nd	nd	nd	nd		
FLVTC5c	Av1	8	1.500	1.068	0.357	0.160	0.091	0.025	6.481	11.013
	Av2	10	2.417	0.795	0.391	0.398	0.089	0.050	**7.886**	**13.400**
	2Btj	25	0.250	0.774	0.357	0.178	0.078	0.026	6.711	11.404
	3Btjk	40	0.167	0.929	0.368	0.263	0.072	0.034	**7.778**	**13.218**
	4Bk1	55	0.417	0.860	0.323	0.145	0.066	0.024	6.158	10.464
	5Bk2	70	0.500	0.797	0.349	0.222	0.074	0.038	5.799	9.855
	6BCk	95	0.250	0.853	0.370	0.325	0.079	0.046	7.052	11.983
	7CB	110	0.333	0.735	0.327	0.306	0.073	0.037	**8.344**	**14.179**
	8C	120	0.333	0.779	0.306	0.212	0.070	0.031	6.751	11.472
	9Bb	135	0.167	0.778	0.349	0.293	0.087	0.051	5.744	9.761
FLV-6a	Av	10	0.500	0.608	0.304	0.295	0.080	0.037	8.011	13.613
	Bw	19	0.250	0.629	0.308	0.334	0.071	0.037	8.919	15.156
	Bt	29	1.000	0.566	0.334	0.357	0.064	0.032	11.320	19.236
	Bk1	42	0.667	0.447	0.304	0.567	0.056	0.045	**12.551**	**21.329**
	2Bk2	52	1.250	0.612	0.332	0.468	0.061	0.040	11.639	19.778
	3Bz	87	0.000	0.702	0.501	0.451	0.097	0.054	8.381	14.241
	4Bwb	107	0.000	0.763	0.419	0.361	0.090	0.042	8.656	14.710
	5BC	137	0.000	0.724	0.342	0.276	0.073	0.037	7.527	12.791
FLV-7b	A	4	0.000	0.597	0.293	0.193	0.084	0.030	6.367	10.820
	2C1	20	0.333	0.573	0.364	0.190	0.084	0.032	5.997	10.191
	3C2	50	0.250	0.814	0.396	0.351	0.097	0.038	**9.236**	**15.695**
	4C3	63	0.000	0.686	0.293	0.302	0.080	0.042	7.222	12.273
	5C4	78	0.167	0.597	0.329	0.389	0.083	0.049	**8.016**	**13.622**
	6C5	98	0.333	0.751	0.304	0.240	0.079	0.035	6.890	11.709
FLV-8A	channel			0.879	0.494	0.351	0.385	0.259	1.355	2.303
max of column			13.667	1.402	0.646	1.803	0.385	0.170	10.603	18.018